Progress in atomic layer deposited α-Ga_2O_3 materials and solar-blind detectors

F.C-P. Massabuau[a], J.W. Roberts[b], D. Nicol[a], P.R. Edwards[a], M. McLelland[a], G.L. Dallas[a], D.A. Hunter[a], E.A. Nicolson[a], J.C. Jarman[c], A. Kovács[d], R.W. Martin[a], R.A. Oliver[c], and P.R. Chalker[b]

[a]Department of Physics, SUPA, University of Strathclyde, Glasgow G4 0NG, UK
[b]School of Engineering, The University of Liverpool, Liverpool L69 3GH, UK
[c]Department of Materials Science and Metallurgy, University of Cambridge, Cambridge CB3 0FS, UK
[d]Ernst Ruska-Centre for Microscopy and Spectroscopy with Electrons and Peter Grünberg Institute, Forschungszentrum Jülich, 52425 Jülich, Germany

ABSTRACT

Atomic layer deposition (ALD) offers a low thermal budget method for producing α-Ga_2O_3 films on sapphire substrate. In this paper we review the recent progress on plasma-enhanced ALD growth of α-Ga_2O_3 and present the optical and photoconductive properties of the deposited films. We show that the deposited material exhibits an epitaxial relationship with the sapphire substrate, and with an atomically sharp film-substrate interface. The α-Ga_2O_3 films had an optical bandgap energy measured at 5.11 eV, and exhibited a broad luminescence spectrum dominated by ultraviolet, blue and green bands, in line with current literature. We finally demonstrate the suitability of the material for solar-blind photodetection.

Keywords: Gallium oxide, Corundum phase, Atomic layer deposition, Solar-blind detection

1. INTRODUCTION

Gallium oxide (Ga_2O_3) has recently emerged as a wide bandgap semiconductor with promising applications for high power and high frequency electronics, as well as ultraviolet optoelectronics.[1] This compound is a polymorphic sesquioxide, with reported phases labelled α, β, ϵ, κ, and γ[2,3] – with the ϵ and κ phases being ordered and disordered variants.[4] The monoclinic β-Ga_2O_3 is the only thermodynamically stable polymorph, and has therefore attracted most research interest to date. The rhombohedral α-phase is metastable, but presents several assets for device applications. For example α-Ga_2O_3 exhibits the widest bandgap energy (*ca.* 5-5.3 eV[5–8]) amongst all phases of Ga_2O_3, making it interesting for power electronic applications. Moreover, it is isostructural with several other semiconducting sesquioxides, therefore exhibiting much promise for bandgap and functionality engineering through alloying with *e.g.* Al_2O_3,[9] In_2O_3,[9] Cr_2O_3,[10] Fe_2O_3,[11] Ti_2O_3,[12] or Rh_2O_3.[13]

Due to its metastability, progress in α-Ga_2O_3 synthesis only arose recently. In recent years, films of α-Ga_2O_3 have successfully been deposited at temperatures in the range of 550-700 °C using mist chemical vapour deposition (mist-CVD),[5,9] halide vapour phase epitaxy (HVPE),[14–16] metalorganic chemical vapour deposition (MOCVD),[6,17] or molecular beam epitaxy (MBE).[18,19] In comparison, plasma-enhanced atomic layer deposition (PEALD)[7,8,20–22] allows the deposition of crystalline α-Ga_2O_3 material at much lower temperatures, nearing 250-300 °C. In this paper we review the conditions for growing α-phase Ga_2O_3 by PEALD and present the optical and photoelectric properties of the films.

F.M.: E-mail: f.massabuau@strath.ac.uk

2. METHODS

Undoped Ga_2O_3 films were deposited on *c*-plane sapphire substrates with a 0.25 ± 0.10° miscut towards $(11\bar{2}0)$ using an Oxford Instruments OpAL PEALD reactor. Adduct grade triethylgallium (TEGa) and dry O_2 were used as the gallium and oxygen sources, respectively, while argon was used for chamber purges and as the precursor carrier gas. Several sets of samples were grown, to investigate the impact of substrate temperature, O_2 flow rate and plasma power on the crystallinity of the Ga_2O_3 films. Table 1 lists the experimental conditions used in each set.

The following conditions were kept constant between growth sets: 0.1 s TEGa dose, 5 s TEGa purge, 5 s O_2 plasma duration, 5 s O_2 plasma purge. 100 sccm Ar was used as a carrier gas during the TEGa dose and to remove unreacted precursors from the chamber during the purge steps. The base pressure in the chamber (with no process gases flowing) was *ca.* 10 mTorr. During the deposition processes the chamber pressure varied between *ca.* 80 mTorr (during the plasma steps) and 160 mTorr (during the TEGa dose). The TEGa source was maintained at 30°C, with line temperatures into the reactor chamber held at 80°C and 90°C. For the lowest temperature deposition (120°C substrate) the chamber walls were held at 125°C, while the chamber walls were set at 150°C for all other growths. 500 cycles were used for the growth of each film, resulting in a film thickness of approximately 25 nm. Finally, a thicker sample (4700 cycles, *ca.* 250 nm thick) was deposited using the optimal conditions listed in Table 1.

The structure of the samples was investigated by X-ray diffraction (XRD) using a PANalytical Empyrean diffractometer with a Cu Kα_1 X-ray source. A two-bounce Ge analyser was used for 2θ-ω scans, and a PIXcel detector was used to acquire reciprocal space maps. The atomic structure of the samples was observed using high-angle annular dark-field scanning transmission electron microscopy (HAADF-STEM) in an aberration-corrected FEI Titan operated at 200 kV.[23] The optical bandgap of the material was obtained using a Shimadzu UV-2600 UV-vis transmittance spectrophotometer equipped with an integrating sphere. The luminescence properties were obtained using room temperature cathodoluminescence (CL) in a JEOL JXA-8530F field-emission electron probe microanalyser (EPMA) operated at 5 kV. Finally, photoelectric characterisation was performed using a Signatone probe station equipped with a Thorlabs Deuterium light source coupled to a SolarLS ML44 monochromator to illuminate the sample with a monochromatic light.

3. RESULTS AND DISCUSSION

3.1 Growth

The impact of the substrate temperature, O_2 flow and plasma power on the resulting phase of the thin films was investigated by means of XRD. The results are summarised in Figure 1. The intense peak at $2\theta = 41.68°$ visible in all the diffractograms corresponds to the α-Al_2O_3 0006 reflection from the substrate. The α-Ga_2O_3 0006 reflection occurs near $2\theta = 40.25°$, which is the value for relaxed α-Ga_2O_3.[24] Small deviations in peak

Table 1. Summary of samples sets and growth conditions investigated.

Sample set	Approx. thickness (nm)	Substrate temperature (°C)	O_2 flow (sccm)	O_2 plasma power (W)
Temperature	25	120, 150, 200, 250, 300, 350, 400, 450	20	300
O_2 flow	25	250	10, 20, 40, 60, 100	300
Plasma power	25	250	20	25, 50, 100 200, 300
Optimal	250	250	20	300

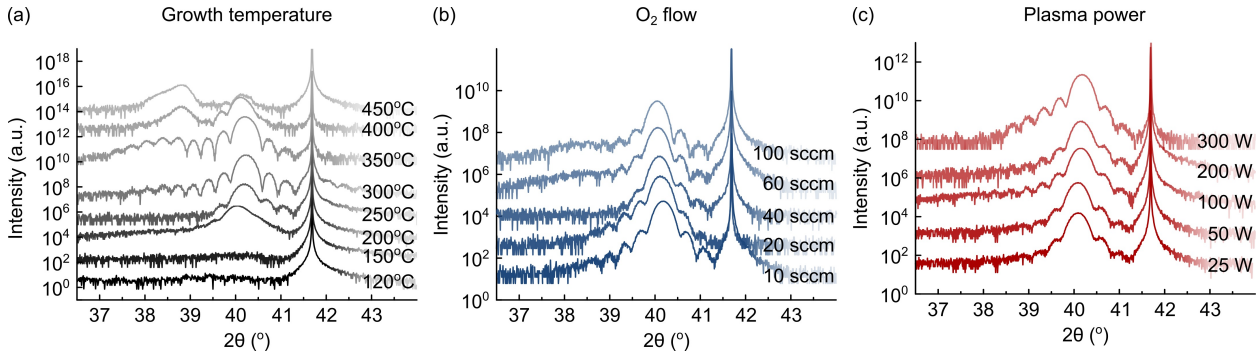

Figure 1. XRD 2θ-ω scans of the samples grown under various (a) temperature, (b) O_2 flow, and (c) plasma power.

position can be ascribed to strain in the film. Peaks occurring at lower angles ($2\theta = 38 - 39°$) correspond to reflections from other phases of Ga_2O_3 – in particular β- and ϵ-Ga_2O_3 exhibit several reflections in that range.

We note that the substrate temperature seems to have the dominant impact on the crystallinity of the deposited film – as illustrated in Figure 1(a). For temperatures below 200°C, no film reflection could be observed, indicating that the films are amorphous. This is in line with previous work which also reported amorphous materials at such low temperatures,[21,25] in particular Borujeny *et al.* identified 190°C as the onset temperature for deposition of crystalline Ga_2O_3 on sapphire by PEALD.[21] For substrate temperatures in the range of 200-350°C, the diffractograms exhibit an α-Ga_2O_3 0006 reflection. Fringes on either side of the peak are indicative of the film thickness and warrant a uniform thickness and good crystalline quality of the deposited material. We find that 250-300°C seems to be the optimal temperature for α-Ga_2O_3 deposition by PEALD. Other studies have also reported α-Ga_2O_3 growth by ALD on sapphire in that temperature window.[8,20–22] For substrate temperatures above 400°C, we observe a noticeable quenching of the intensity of the α-Ga_2O_3 0006 reflection and the appearance of reflections near $2\theta = 38 - 39°$ – in agreement with other studies.[8,21] This is indicative that growth at such temperatures favours the β- and ϵ-phases which are more stable than α-Ga_2O_3.[26]

When grown at 250°C we find that, over the range of values investigated, the O_2 flow and plasma power seem to have a negligible effect on the resulting phase of the film. As seen in Figure 1(b-c) all the films were α-Ga_2O_3. Minor variations in peak position could be ascribed to variations in the strain state of the films. It should be pointed out that this result is in contrast with Wheeler *et al.* who found that the plasma conditions offer wide scope for tuning the phase of the film.[8] We point out, however, that Wheeler *et al.*'s study used different precursors and different pressure during plasma than our present work. The use of PEALD offers even greater possibilities as a study from Ilhom *et al.* recently reported that *in situ* Ar plasma annealing at the end

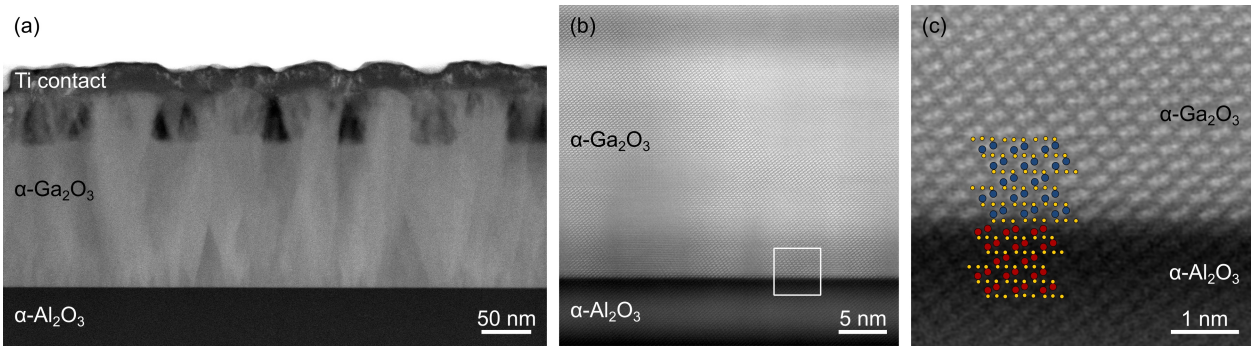

Figure 2. (a) HAADF-STEM image of the film, and (b) film-substrate interface. (c) Zoomed-in image of the region marked by a square in (b), with crystal model overlay (blue: Ga; red: Al; yellow: O). All images were observed along the $\langle 11\bar{2}0 \rangle$ zone axis.

of every PEALD cycle could be used to produce β-phase Ga_2O_3 on sapphire as well as other substrates (Si, glass).[27]

Lastly, we note that the growth of the aforementioned samples was also conducted on silicon substrates, and that all these films deposited on silicon were amorphous. This is in line with earlier literature on Ga_2O_3 deposition by ALD[28–30] (with the exception of Ilhom *et al.* who used an extra plasma step to crystallise the films[27]). This highlights that the sapphire substrate plays a critical role in stabilising the corundum phase – as expected owing to its similar crystal structure and relatively low lattice mistmatch of about 4.8% with α-Ga_2O_3. We illustrate the importance of the sapphire substrate in Figure 2, which depicts cross-sectional aberration-corrected HAADF-STEM images of the thick Ga_2O_3 film. We note the columnar structure of the film, with all columns starting at the film-substrate interface, and propagating though the whole layer (Figure 2(a)). The several columns illustrate the mosaicity of the film, which has also been reported in α-Ga_2O_3 films grown using other methods.[14,31] Regions of different contrast have been identified as amorphous and ϵ-Ga_2O_3 inclusions.[20] Figure 2(b-c) provide high resolution images of the film-substrate interface, where the sharpness of the interface and epitaxial growth of the film on the sapphire substrate can be clearly observed.

3.2 Optical properties

UV-vis transmittance spectroscopy was used to measure the optical bandgap of the thick film. The transmittance of the film in the 200-700 nm wavelength range is presented in Figure 3(a), where a sharp increase in transmittance can be observed in the 230-280 nm region. Using the Tauc plot $(\alpha h\nu)^2$ vs $h\nu$ (inset of Figure 3(a)) to estimate the direct bandgap energy of the film, as is conventionally used with this material,[6–8,14,19] we obtain an optical bandgap of 5.11 eV, which is well within the 5-5.3 eV range of values reported in the literature.[5–8,12,14,19]

Room temperature CL was conducted to assess the luminescence properties of the thick film. The resulting CL spectrum is shown in Figure 3(b). In agreement with the literature, no band edge emission could be observed. Instead, the CL spectrum exhibits a broad emission spectrum from which four main components can be distinguished. We observed bands at 340 nm (*ca.* 3.6 eV), 394 nm (*ca.* 3.1 eV), 465 nm (*ca.* 2.7 eV), 550 nm (*ca.* 2.3 eV), as well as a tail that extends to even longer wavelengths. The CL spectrum present some similarities with the CL data obtained by Polyakov *et al.* on HVPE-grown Sn-doped α-Ga_2O_3.[32] However in our study, the samples are nominally undoped so we would not expect to see strong Sn-related luminescence as any Sn in the film (if any) should be in trace amount. Literature on luminescence of α-Ga_2O_3 is scarce,[32,33] we therefore turn our attention to the literature on β-Ga_2O_3 to try to assess the origin of the luminescence in our sample. Luminescence of β-Ga_2O_3 generally exhibits mainly UV (3.2–3.6 eV), blue (2.8–3.0 eV) and green (2.5 eV) lines,[34–36] but a red (1.7–1.9 eV) line has also been reported.[37–39] The UV line as been ascribed to recombination between free electrons and self-trapped holes (STHs), while the other lines relate to donor acceptor

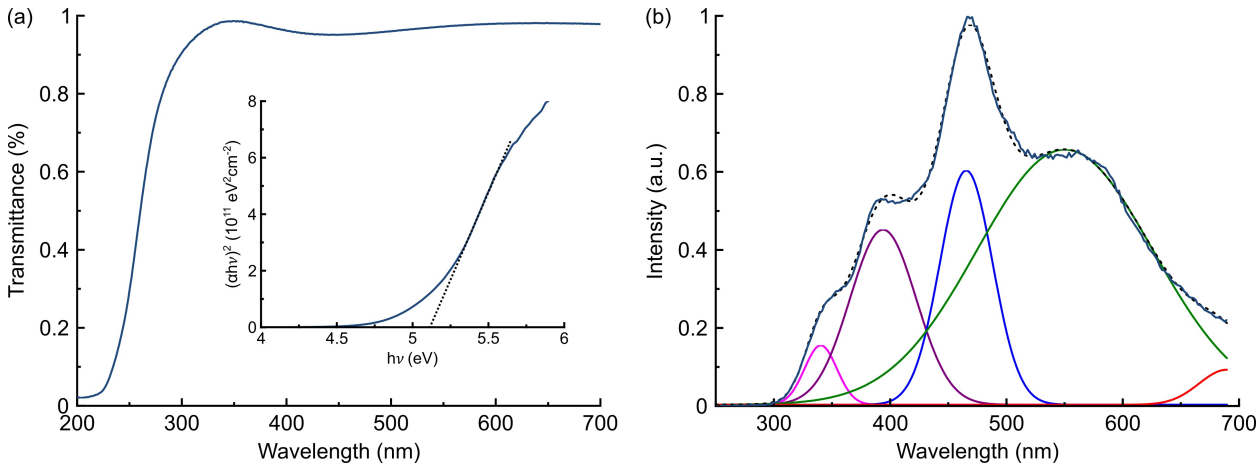

Figure 3. (a) UV-vis transmittance spectrum of the thick α-Ga_2O_3 film, with Tauc plot in inset. (b) Room temperature CL spectrum of the thick α-Ga_2O_3 film.

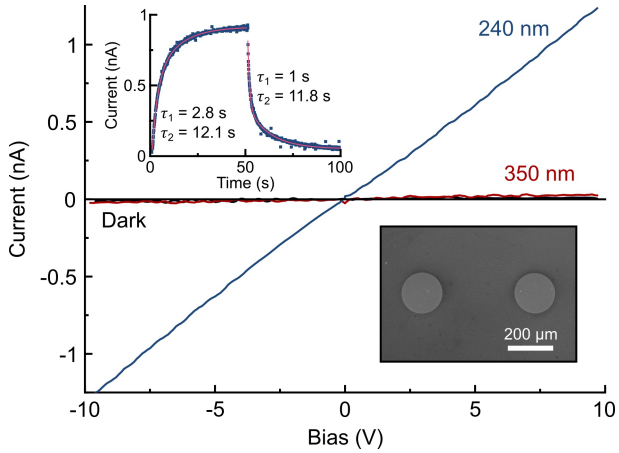

Figure 4. I-V characteristic of the thick α-Ga_2O_3 film tested under 240 nm, 350 nm and dark illumination. In insets, 240 nm photoconduction transient, and scanning electron microscope image of the contact structure used.

pair recombination involving a range of intrinsic (e.g. V_O, V_{Ga}, Ga_i) or extrinsic (e.g. Si_{Ga}, N_O) defects. While we here expect limited contribution from extrinsic defects, the luminescence we observe in Figure 3(b) is aligned with the main luminescence lines reported in β-Ga_2O_3, which we therefore tentatively ascribe to electron-STH recombination (340 nm line) and donor acceptor pair recombinations (394 nm, 465 nm, 550 nm lines). Further work would nevertheless be necessary to ascertain the exact defects involved.

3.3 Solar-blind photodetectors

To test the suitability of the material for solar-blind detection, circular Ti/Au electrodes *ca.* 180 μm in diameter and spaced *ca.* 500 μm apart (as shown in the scanning electron microscopy image in inset of Figure 4) were deposited onto the thick α-Ga_2O_3 film using UV photolithography and thermal evaporation. Figure 4 shows the photocurrent and transient characteristics when the device is illuminated under light at 240 nm, 350 nm, and in the dark. A clear increase in photocurrent can be observed when the film is illuminated by above bandgap light (*i.e.* 240 nm), as opposed to below bandgap illumination (*i.e.* 350 nm) or dark conditions. At 10 V bias, the photocurrent under 240 nm illumination is measured at 1.2 nA for a dark current of *ca.* 6 pA resulting in a photo-to-dark-current-ratio (PDCR) of about 220. It should be noted that the dark current has a low accuracy because it is limited by the source meter's detection limit and noise, moreover the photocurrent could be increased if the electrode structure were optimised (*i.e.* interdigitated electrodes). This result nevertheless demonstrates the suitability of ALD-grown α-Ga_2O_3 for solar-blind sensing. Previous studies on ALD-grown α-Ga_2O_3 photodetectors[22,40] reported responsivities nearing 1 $A.W^{-1}$ that are well within the range of responsivities reported for detectors obtained using different growth methods, and based on other more mature phases of Ga_2O_3.[41]

With regards to time response, our data show a relatively slow rise and decay, but still in agreement with literature values for Ga_2O_3 detectors (all phases included).[41] Using a bi-exponential fit for the rise and decay response (shown in inset of Figure 4) we obtained time constants of 2.8 s and 12.1 s for the fast and slow rise components, respectively, and 1.0 s and 11.8 s for the fast and slow decay components, respectively. The particularly slow response of Ga_2O_3 photodetector devices has been ascribed to an accumulation of STHs at the semiconductor/metal interface.[42,43] It should be noted that Lee *et al.* reported ultrafast, sub-microsecond response time for ALD-grown α-Ga_2O_3-based photodetectors[22] which is amongst the fastest performance obtained so far in the field.

4. CONCLUSION

In this paper we have reviewed the recent progress on the use of PEALD for the growth of α-Ga_2O_3 with a very low thermal budget in comparison to other growth methods. We reported that the temperature, plasma conditions,

and substrate play a determining role in the resulting phase of the film. We went on to present the optical and photoelectric properties of thick α-Ga_2O_3 film grown under the optimal conditions. The optical bandgap energy was measured at 5.11 eV, and CL measurement showed a broad luminescence spectrum consisting of ultraviolet, blue and green bands, in line with current literature. We finally demonstrated that ALD-grown α-Ga_2O_3 films are suitable for solar-blind photodetection and exhibit performances in par with other more mature phases of Ga_2O_3.

ACKNOWLEDGMENTS

The authors acknowledge support from the Royal Society (RGS\R1\201236), the Engineering and Physical Sciences Research Council (EP/T517938/1; EP/V034995/1; EP/P00945X/1; EP/M010589/1; EP/K014471/1), and the European Union's Horizon 2020 research and innovation programme (grant agreement No 823717–ESTEEM3). The data that support the findings of this study are openly available in PurePortal at https://doi.org/10.15129/1776202a-4c26-4c74-8b7b-e9fd2d5a2270 .

REFERENCES

[1] Pearton, S. J., Yang, J., Cary, P., Ren, F., Kim, J., Tadjer, M., and Mastro, M., "A review of Ga_2O_3 materials, processing, and devices," *Applied Physics Reviews* **5**(1), 011301 (2018).

[2] Roy, R., Hill, V., and Osborn, E., "Polymorphism of Ga_2O_3 and the system Ga_2O_3-H_2O," *Journal of the American Chemical Society* **74**(3), 719 (1952).

[3] Playford, H., Hannon, A., Barney, E., and Walton, R., "Structures of uncharacterised polymorphs of gallium oxide from total neutron diffraction," *Chemistry – A European Journal* **19**(8), 2803–2813 (2013).

[4] Cora, I., Mezzadri, F., Boschi, F., Bosi, M., Caplovicova, M., Calestani, G., Dodony, I., Pecz, B., and Fornari, R., "The real structure of ϵ-Ga_2O_3 and its relation to κ-phase," *Crysl Eng Comm* **19**, 1509 (2017).

[5] Shinohara, D. and Fujita, S., "Heteroepitaxy of corundum-structured α-Ga_2O_3 thin films on α-Al_2O_3 substrates by ultrasonic mist chemical vapor deposition," *Japanese Journal of Applied Physics* **47**, 7311 (2008).

[6] Sun, H., Li, K.-H., Torres Castanedo, C., Okur, S., Tompa, G., Salagaj, T., Lopatin, S., Genovese, A., and Li, X., "Hcl flow-induced phase change of α-, β-, and ϵ-Ga_2O_3 films grown by mocvd," *Crystal Growth and Design* **18**, 2370 (2018).

[7] Roberts, J., Chalker, P., Ding, B., Oliver, R., Gibbon, J., Jones, L., Dhanak, V., Phillips, L., Major, J., and Massabuau, F.-P., "Low temperature growth and optical properties of α-Ga_2O_3 deposited on sapphire by plasma enhanced atomic layer deposition," *Journal of Crystal Growth* **528**, 125254 (2019).

[8] Wheeler, V., Nepal, N., Boris, D., Qadri, S., Nyakiti, L., Lang, A., Koehler, A., Foster, G., Walton, S., Eddy, C., and Meyer, D., "Phase control of crystalline Ga_2O_3 films by plasma-enhanced atomic layer deposition," *Chemistry of Materials* **32**(3), 1140–1152 (2020).

[9] Fujita, S. and Kaneko, K., "Epitaxial growth of corundum-structured wide bandgap III-oxide semiconductor thin films," *Journal of Crystal Growth* **401**, 588 (2014).

[10] Kaneko, K., Nomura, T., and Fujita, S., "Corundum-structured α-phase Ga_2O_3-Cr_2O_3-Fe_2O_3 alloy system for novel functions," *Physica Status Solidi C* **7**, 2467 (2010).

[11] Kaneko, K., Nomura, T., Kakeya, I., and Fujita, S., "Fabrication of highly crystalline corundum-structured α-$(Ga_{1-x}Fe_x)_2O_3$ alloy thin films on sapphire substrates," *Applied Physics Express* **2**, 075501 (2009).

[12] Barthel, A., Roberts, J., Napari, M., Frentrup, M., Huq, T., Kovacs, A., Oliver, R., Chalker, P., Sajavaara, T., and Massabuau, F., "Ti alloyed α-Ga_2O_3: Route towards wide band gap engineering," *Micromachines* **11**(12), 1128 (2020).

[13] Kaneko, K., Fujita, S., and Hitora, T., "A power device material of corundum-structured α-Ga_2O_3 fabricated by mist epitaxy technique," *Japanese Journal of Applied Physics* **57**, 02CB18 (2018).

[14] Oshima, Y., Víllora, E., and Shimamura, K., "Halide vapor phase epitaxy of twin-free α-Ga_2O_3 on sapphire (0001) substrates," *Applied Physics Express* **8**, 055501 (2015).

[15] Pechnikov, A.I., S. S. C. A., Scheglov, M., Odnobludov, M., and Nikolaev, V., "Thick α-Ga_2O_3 layers on sapphire substrates grown by halide epitaxy," *Semiconductors* **53**, 780 (2019).

[16] Lee, M., Yang, M., Lee, H.-Y., Lee, H., Lee, H., Son, H., and Kim, U., "The growth of hvpe α-Ga_2O_3 crystals and its solar-blind uv photodetector applications," *Materials Science in Semiconductor Processing* **123**, 105565 (2021).

[17] Gottschalch, V., Merker, S., Blaurock, S., Kneiss, M., Teschner, U., Grundmann, M., and Krautscheid, H., "Heteroepitaxial growth of α-, β-, γ- and κ-Ga_2O_3 phases by metalorganic vapor phase epitaxy," *Journal of Crystal Growth* **510**, 76 (2019).

[18] Kumaran, R., Tiedje, T., Webster, S., Penson, S., and Li, W., "Epitaxial nd-doped α-$(Al_{1-x}Ga_x)_2O_3$ films on sapphire for solid-state waveguide lasers," *Optics Letters* **35**, 3793 (2010).

[19] Guo, D., Zhao, X., Zhi, Y., Cui, W., ., Huang, Y., An, Y., Li, P., Wu, Z., and Tang, W., "Epitaxial growth and solar-blind photoelectric properties of corundum-structured α-Ga_2O_3 thin films," *Materials Letters* **164**, 364 (2016).

[20] Roberts, J., Jarman, J., Johnstone, D., Midgley, P., Chalker, P., Oliver, R., and Massabuau, F.-P., "α-Ga_2O_3 grown by low temperature atomic layer deposition on sapphire," *Journal of Crystal Growth* **487**, 23 – 27 (2018).

[21] Rafie Borujeny, E., Sendetskyi, O., Fleischauer, M., and Cadien, K., "Low thermal budget heteroepitaxial gallium oxide thin films enabled by atomic layer deposition," *ACS Applied Materials & Interfaces* **12**(39), 44225–44237 (2020).

[22] Lee, S., Lee, K., Kim, Y.-B., Moon, Y.-J., Kim, S., Bae, D., Kim, T., Kim, Y., Kim, S., and Lee, S., "Sub-microsecond response time deep-ultraviolet photodetectors using α-Ga_2O_3 thin films grown via low-temperature atomic layer deposition," *Journal of Alloys and Compounds* **780**, 400 – 407 (2019).

[23] Kovacs, A., Schierholz, R., and Tillmann, K., "FEI TITAN G2 80-200 CREWLEY," *Journal of large-scale research facilities* **2**, A43 (2016).

[24] Marezio, M. and Remeika, J., "Bond lengths in the α-Ga_2O_3 structure and the high-pressure phase of $Ga_{2-x}Fe_xO_3$," *The Journal of Chemical Physics* **46**(5), 1862–1865 (1967).

[25] Hong, T., Choi, W.-H., Choi, S.-H., Lee, H., Seok, J., Park, J., Lim, J., and Park, J.-S., "Plasma enhanced atomic layer deposited amorphous gallium oxide thin films using novel trimethyl[n-(2-methoxyethyl)-2-methylpropan-2-amine]gallium," *Ceramics International* **47**(2), 1588 – 1593 (2021).

[26] Yoshioka, S., Hayashi, H., Kuwabara, A., Oba, F., Matsunaga, K., and Tanaka, I., "Structures and energetics of Ga_2O_3 polymorphs," *Journal of Physics: Condensed Matter* **19**(34), 346211 (2007).

[27] Ilhom, S., Mohammad, A., Shukla, D., Grasso, J., Willis, B., Okyay, A., and Biyikli, N., "Low-temperature as-grown crystalline β-Ga_2O_3 films via plasma-enhanced atomic layer deposition," *ACS Applied Materials and Interfaces* (2019).

[28] Shih, H.-Y., Chu, F.-C., Das, A., Lee, C.-Y., Chen, M.-J., and Lin, R.-M., "Atomic layer deposition of gallium oxide films as gate dielectrics in AlGaN/GaN metal–oxide–semiconductor high-electron-mobility transistors," *Nanoscale Research Letters* **11**, 235 (2016).

[29] Donmez, I., Ozgit-Akgun, C., and Biyikli, N., "Low temperature deposition of Ga_2O_3 thin films using trimethylgallium and oxygen plasma," *J. Vac. Sci. Technol. A* **31**, 01A110 (2013).

[30] Comstock, D. and Elam, J., "Atomic layer deposition of Ga_2O_3 films using trimethylgallium and ozone," *Chemistry of Materials* **24**, 4011 (2012).

[31] Fujita, S., Oda, M., Kaneko, K., and Hitora, T., "Evolution of corundum-structured iii-oxide semiconductors: Growth, properties, and devices," *Japanese Journal of Applied Physics* **55**, 1202A3 (2016).

[32] Polyakov, A., Smirnov, N., Shchemerov, I., Yakimov, E., Nikolaev, V., Stepanov, S., Pechnikov, A., Chernykh, A., Shcherbachev, K., Shikoh, A., Kochkova, A., Vasilev, A., and Pearton, S., "Deep trap spectra of sn-doped α-Ga_2O_3 grown by halide vapor phase epitaxy on sapphire," *APL Materials* **7**, 051103 (2019).

[33] Cho, S., Lee, J., Park, I. Y., and Kim, S., "Temperature dependence of photoluminescence of α-Ga_2O_3 powders," *Japanese Journal of Applied Physics* **41**, 5237 (2002).

[34] Onuma, T., Nakata, Y., Sasaki, K., Masui, T., Yamaguchi, T., Honda, T., Kuramata, A., Yamakoshi, S., and Higashiwaki, M., "Modeling and interpretation of uv and blue luminescence intensity in β-Ga_2O_3 by silicon and nitrogen doping," *Journal of Applied Physics* **124**(7), 075103 (2018).

[35] Onuma, T., Fujioka, S., Yamaguchi, T., Higashiwaki, M., Sasaki, K., Masui, T., and Honda, T., "Correlation between blue luminescence intensity and resistivity in β-Ga_2O_3 single crystals," *Applied Physics Letters* **103**(4), 041910 (2013).

[36] Villora, E., Yamaga, M., Inoue, T., Yabasi, S., Masui, Y., Sugawara, T., and Fukuda, T., "Optical spectroscopy study on β-Ga_2O_3," *Japanese Journal of Applied Physics* **41**, L622–L625 (2002).

[37] Ho, Q., Frauenheim, T., and Deak, P., "Origin of photoluminescence in β-Ga_2O_3," *Physical Review B* **97**, 115163 (2018).

[38] Huynh, T., Chikoidze, E., Irvine, C., Zakria, M., Dumont, Y., Teherani, F., Sandana, E., Bove, P., Rogers, D., Phillips, M., and Ton-That, C., "Red luminescence in h-doped β-Ga_2O_3," *Physical Revview Materials* **4**, 085201 (2020).

[39] Gunasekar, N., MacIntyre, H., Subashchandran, S., Edwards, P., Martin, R., Daivasigamani, K., Sasaki, K., and Kuramata, A., "Origin of red emission in β-Ga_2O_3 analyzed by cathodoluminescence and photoluminescence spectroscopy," *Physica Status Solidi B* **258**, 2000465 (2021).

[40] Moloney, J., Tesh, O., Singh, M., Roberts, J., Jarman, J., Lee, L., Huq, T., Brister, J., Karboyan, S., Kuball, M., Chalker, P., Oliver, R., and Massabuau, F. C.-P., "Atomic layer deposited α-Ga_2O_3 solar-blind photodetectors," *Journal of Physics D: Applied Physics* **52**(47), 475101 (2019).

[41] Hou, X., Zou, Y., Ding, M., Qin, Y., Zhang, Z., Ma, X., Tan, P., Yu, S., Zhou, X., Zhao, X., Xu, G., Sun, H., and Long, S., "Review of polymorphous Ga_2O_3 materials and their solar-blind photodetector applications," *Journal of Physics D: Applied Physics* **54**(4), 043001 (2020).

[42] Xu, Y., Chen, X., Zhou, D., Ren, F., Zhou, J., Bai, S., Lu, H., Gu, S., Zhang, R., Zheng, Y., and Ye, J., "Carrier transport and gain mechanisms in β-Ga_2O_3-based metal-semiconductor-metal solar-blind schottky photodetectors," *IEEE Transactions on Electron Devices* **66**, 2276 (2019).

[43] Armstrong, A., Crawford, M., Jayawardena, A., Ahyi, A., and Dhar, S., "Role of self-trapped holes in the photoconductive gain of β-gallium oxide schottky diodes," *Journal of Applied Physics* **119**, 103102 (2016).